



Enhancement of cell performance using a gadolinium strontium cobaltite coated cathode in molten carbonate fuel cells

Shin Ae Song, Seong-Cheol Jang, Jonghee Han*, Sung Pil Yoon, Suk Woo Nam, In-Hwan Oh, Tae-Hoon Lim

Fuel Cell Research Center, Korea Institute of Science and Technology, 39-1 Hawolgok-dong, Seongbuk-gu, Seoul 136-791, Republic of Korea

ARTICLE INFO

Article history:

Received 27 April 2011

Received in revised form 20 July 2011

Accepted 5 August 2011

Available online 12 August 2011

Keywords:

Molten carbonate fuel cells

Gadolinium strontium cobaltite coated cathode

High performance

Reduction of cathode polarization

ABSTRACT

To enhance cathode performance, gadolinium strontium cobaltite ($\text{Gd}_{0.6}\text{Sr}_{0.4}\text{CoO}_3$, GSC) is coated onto a porous Ni plate by a vacuum suction method, for use as the cathode in molten carbonate fuel cells (MCFCs). GSC is a mixed ionic and electronic conductor (MIEC) material, and thus has high electronic conductivity and catalytic activity at low temperatures. The electrode performance of the GSC-coated cathode is examined by various methods, such as single cell operation and electrochemical impedance spectroscopy (EIS). At 600 °C, the performance of a single cell using a GSC-coated cathode is 0.813 V. This result is very surprising given that the performance of an uncoated conventional cathode is 0.69 V. Impedance analysis confirms that a dramatic decrease in the charge transfer resistance after GSC coating is primarily responsible for the cell enhancement at low temperature. The reaction orders for O_2 and CO_2 at uncoated and GSC-coated cathodes are also examined via a symmetric cell test, to identify the reaction mechanism of oxygen reduction. The peroxide mechanism, which is known to be a fast reaction, is predominant for the GSC-coated cathode at low temperatures, whereas the superoxide mechanism is predominant for the uncoated cathode.

© 2011 Elsevier B.V. All rights reserved.

1. Introduction

Fuel cells have received much attention as next-generation electricity production systems, due to their high efficiency and negligible emissions. Among many types of fuel cells, molten carbonate fuel cells (MCFCs) operated at a high temperature (650 °C) have been developed for decades, and will soon enter the initial stage of commercialization. These fuel cells are highly efficient, do not require expensive noble metal catalysts, and have a variety of usable fuels [1–3]. MCFCs do, however, have a number of problems that must be solved in order for these cells to compete with current commercially available power generation devices, such as diesel engines and gas turbines. One of the most serious problems is guaranteeing the long-term lifetime of MCFC stacks [4–6]. The commercial target for the lifetime of a MCFC stack is more than 40,000 h, but this goal has not yet been reached with a single stack.

The main obstacle to reaching a 40,000 h lifetime is electrolyte loss caused by the volatilization and corrosion of the metallic separators [7]. An easy way to suppress electrolyte loss is to operate the MCFC stack at a low temperature, as this reduces the volatilization of the electrolyte and makes the corrosion reaction slow, thus

suppressing the electrolyte loss. MCFCs operated at low temperatures, however, have low stack performance, primarily because of reduced ionic conductivity in the electrolyte and the slow rate of the electrode reaction [8]. It is well known that the oxygen reduction reaction (ORR) rate at the cathode slows down when the operating temperature is decreasing, and a slow cathodic reaction leads to large over-potentials at the cathode, causing the low cell performance at low temperature. In contrast, the hydrogen oxidation reaction at the anode is a relatively fast reaction at low operating temperatures. Thus, the development of many alternative materials is required to enhance the electrochemical performance of the cathode in MCFC systems. To date, however, very few alternative materials for MCFC cathodes have been reported.

In solid oxide fuel cells (SOFCs), research on reducing the operating temperature is also a major issue in enhancing the chemical, physical, thermal, and mechanical durability of components such as the interconnectors, electrodes, electrolytes, and sealants. Reducing the operating temperature also results in low electrochemical performance in the cathode. Therefore, new cathode materials for operation at 600–800 °C have been widely studied in order to enhance the electrochemical performance of the cathode [9–16]. Among the many potential cathode materials for intermediate temperature solid oxide fuel cells (IT-SOFCs), mixed ionic and electronic conductors (MIECs), which have a perovskite structure such as $\text{La}_x\text{Sr}_{1-x}\text{Co}_y\text{Fe}_{1-y}\text{O}_3$, $\text{Ba}_x\text{Sr}_{1-x}\text{Co}_y\text{Fe}_{1-y}\text{O}_3$, and $\text{Gd}_x\text{Sr}_{1-x}\text{CoO}_3$,

* Corresponding author. Tel.: +82 2 958 5277; fax: +82 2 958 5199.
E-mail address: jhan@kist.re.kr (J. Han).

have received much attention because of their high ionic and electronic conductivities, and their high catalytic activity for electrochemical reactions [10–16]. In particular, $Gd_xSr_{1-x}CoO_3$ has a high conductivity at low temperatures, and a high electrochemical catalytic activity for the cathode reaction of SOFCs. $Gd_{0.5}Sr_{0.5}CoO_3$ has a higher conductivity, at over 540 Scm^{-1} at 600°C , than that of $La_xSr_{1-x}Co_yFe_{1-y}O_3$, which is typically used as the cathode in IT-SOFCs [17]. Thus, $Gd_xSr_{1-x}CoO_3$ has been studied intensively as a cathode material for IT-SOFCs in recent years. For these reasons, $Gd_xSr_{1-x}CoO_3$ is also expected to enhance cathode performance when it is applied to the cathode of MCFCs. In this study, a modified cathode for MCFCs was prepared by coating $Gd_xSr_{1-x}CoO_3$ powder onto a conventional lithiated NiO cathode, and the electrode properties of the prepared cathode in an MCFC system were tested.

2. Experimental

A modified cathode was prepared by coating GSC powder ($Gd_{0.6}Sr_{0.4}CoO_3$, Newell, Inc., South Korea) onto a conventional lithiated NiO cathode. The GSC powder was coated onto a porous Ni plate, which becomes a lithiated NiO cathode after an in-situ oxidation and lithiation process in the single cell. The porous Ni plates were prepared by a tape casting method, and were then coated with GSC powder using a vacuum suction method. The GSC suspension was prepared as follows. Disperbyk-190 (Daehan, Inc., South Korea) at 3 wt.%, a dispersion agent, was dissolved in ethanol, and the prepared solution was agitated for 30 min. Then, 10 wt.% of the GSC powder, relative to the mass of the Ni plate, was added to the prepared solution, and was dispersed by ultrasonication for 1 h. The prepared GSC suspension was slowly dropped onto the Ni plate, which was then placed on a Buchner funnel connected to a vacuum pump before being dried in an oven at 100°C for 2 h. The final amount of GSC coating on the Ni plate was approximately 4.7 wt.%.

The physical properties of the coated cathode were characterized by various methods. The morphology of the coated cathode was examined by scanning electron microscopy (SEM; NOVA NanoSEM200), and the phase structure of the cathode was analyzed by X-ray diffraction (XRD; RIGAKU) using Cu-K α radiation.

The electrode performance of the GSC-coated cathodes was evaluated in a single cell with an active electrode area of 100 cm^2 . Conventional components, such as a Ni–5 wt.% Al anode, a $Li_{0.62}/K_{0.38}$ carbonate electrolyte, and an $\alpha\text{-LiAlO}_2$ matrix, were used for the single cell test, and the GSC-coated cathodes and conventional uncoated lithiated NiO cathodes were tested in single cells. The performance of each single cell was monitored. The detailed operating conditions of the single cells have been reported previously in the literature [18]. Under the standard operating conditions, a mixture of air and CO_2 was used as the cathode gas, and the fuel gas was a mixture of H_2 , H_2O , and CO_2 . The flow rate of the reaction gas was fixed at 0.4 for fuel and air utilization in the anode and cathode gases. The H_2O in the anode gas was supplied using a water bubbler set to 50°C , and the DC current was applied to the single cells using an electric loader (ELTO DC Electronics Co., ESL300Z). The cell performance was evaluated by measuring the cell voltage at various current densities. To understand the electrochemical characteristics, a symmetric cell test was also performed. A symmetric cell was assembled using two of the same cathodes, matrices, and electrolytes with an area of 25 cm^2 . To analyze the electrode polarization, electrochemical impedance spectroscopy (EIS) analysis was carried out at different operation conditions, using a Solartron SI1287 and a Solartron 1255B. The frequency range of the present EIS experiment was from 10,000 to 0.01 Hz.

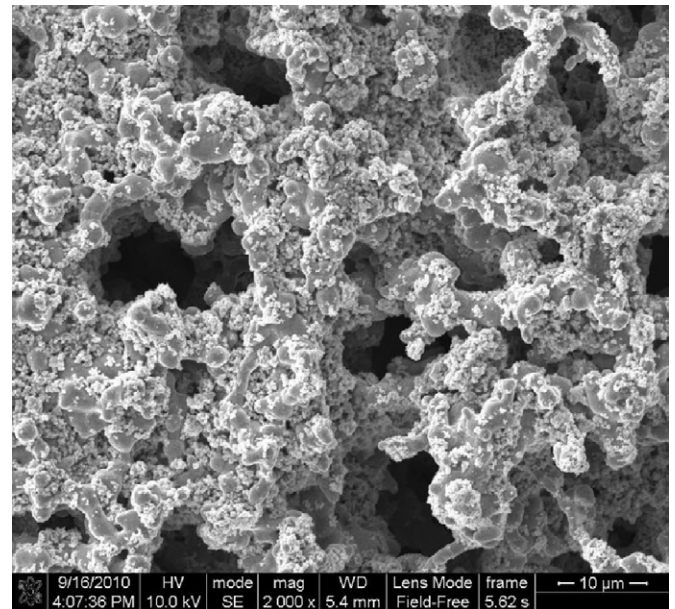


Fig. 1. SEM image of a 4.7 wt.% GSC-coated Ni plate.

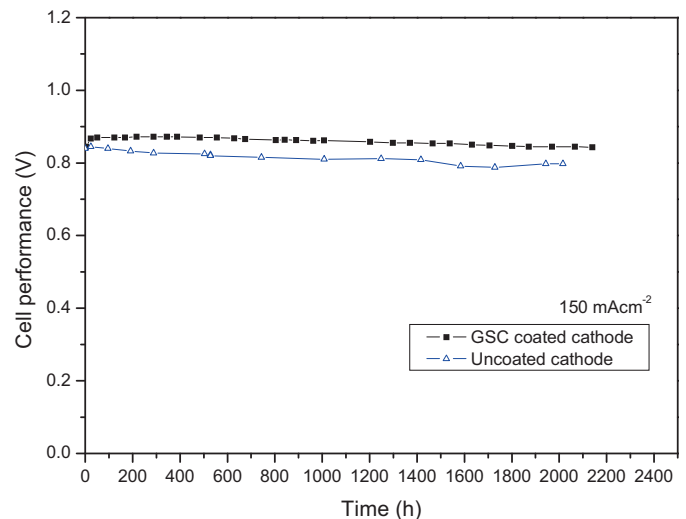


Fig. 2. The variation in the cell performance of single cells containing an uncoated cathode or a GSC-coated cathode operated at a current density of 150 mA cm^{-2} and a temperature of 650°C with standard anode and cathode gas compositions.

3. Results and discussion

The GSC-coated cathode was successfully prepared by a vacuum suction method. The top-view SEM image of a 4.7 wt.% GSC-coated Ni plate is shown in Fig. 1. This shows that small particles of GSC are well deposited on the top and inner surfaces of the porous Ni plate, without forming a thin layer of coating material.

The electrode performance of the GSC-coated cathode was evaluated using single cells. The performance and operating times of single cells using the GSC-coated cathode and the uncoated cathode, operated using standard cathode and anode gas compositions ($U_f = U_o = 0.4$) at 650°C , are shown in Fig. 2. The cells operated at a current density of 150 mA cm^{-2} throughout. As shown in Fig. 2, the cell using the GSC-coated cathode has operated stably for approximately 2200 h, with a high cell performance averaging 0.85 V and no rapid drop off. The cell using the uncoated cathode also has operated very stably, with an average cell performance of 0.82 V for 2200 h. Thus, the GSC coating on the conventional cathode

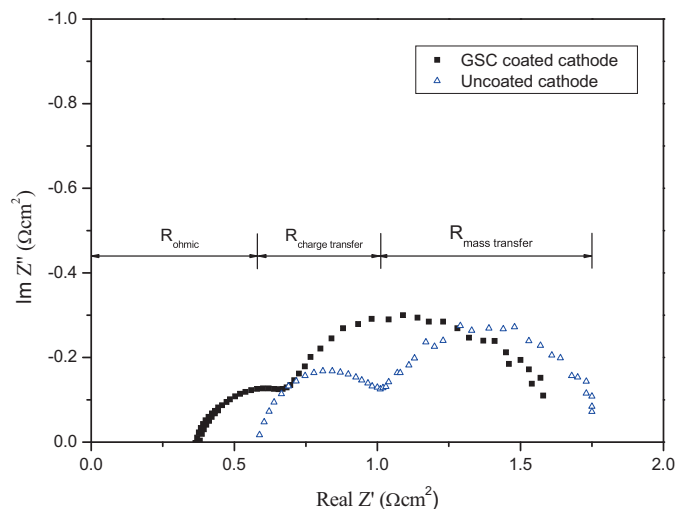


Fig. 3. The Nyquist plots from EIS analysis of single cells containing an uncoated cathode or a GSC-coated cathode at 650 °C with standard anode and cathode gas compositions.

enhances the cell performance, and the GSC-coated cathode is able to operate stably for a long period of time. The high cell performance and 2200 h of stable operation demonstrate that GSC is a very promising material for coating MCFC cathodes.

The impedance spectra of single cells, using GSC-coated cathodes and uncoated cathodes at 650 °C, are presented in Fig. 3. These spectra have intercepts on the real axis, indicating ohmic resistance, and the spectra contain both high- and low-frequency arcs. Although there is some discussion about the meaning of the arcs in impedance spectra for MCFCs, it is generally known that the widths of the high- and low-frequency arcs correlate to the charge transfer resistance and the mass transfer resistance in the electrode, respectively [19]. The ohmic, charge transfer, and mass transfer resistances extracted from Fig. 3 are shown in Table 1. Interestingly, the ohmic resistance and charge transfer resistance are lower after GSC coating, while the mass transfer resistance is higher. As shown in Fig. 3 and Table 1, the enhancement of the cell performance after GSC coating results from the decreases in the ohmic and charge transfer resistances. The large decrease in the charge transfer resistance after GSC coating indicates that the ORR at the cathode is faster, because the operation conditions and cell components, except for the cathode, are identical in each case. The reduction in the charge transfer and ohmic resistances might be caused by the high electronic conductivity of GSC. GSC has a much higher electronic conductivity at 600 °C (greater than 400 Scm^{-1} [17]) than that of lithiated NiO (greater than 10 Scm^{-1} [20]). The rate-determining step of the ORR at the cathode is known to be the reduction step of the superoxide ion or the peroxide ion in carbonate melts receiving an electron transferred from the electrode [21]. The highly electrically conductive GSC may have increased the speed of the rate-determining step of the ORR, and reduced the cathode polarization.

The current density (j)-voltage (V) and current density (j)-power density (P) characteristics of the single cells, using the

Table 1

Comparison of the resistances from EIS analysis of single cells containing uncoated cathodes and GSC-coated cathodes at 650 °C using standard anode and cathode gas compositions.

	R_{ohmic} (Ωcm^2)	$R_{\text{charge transfer}}$ (Ωcm^2)	$R_{\text{mass transfer}}$ (Ωcm^2)
Uncoated cathode	0.57	0.44	0.74
GSC-coated cathode	0.36	0.33	0.88

uncoated and GSC-coated cathodes, in the temperature range 600–700 °C are presented in Fig. 4(a). It is interesting that the cell voltages of the single cell using a 4.7 wt.% GSC-coated cathode were higher than those using an uncoated cathode at all current densities and temperatures. The maximum power densities of the single cell using the GSC-coated cathode are 159, 189, and 204 mW cm^{-2} , at current densities of 280, 300, and 300 mA cm^{-2} and temperatures of 600, 650, and 700 °C, respectively, whereas the maximum power densities of the single cell using the uncoated cathode are 117, 157, and 184 mW cm^{-2} at current densities of 250, 280, and 300 mA cm^{-2} and temperatures of 600, 650, and 700 °C, respectively. The performance of the cathode modified by GSC coating is dramatically improved compared to that of the conventional cathode in the measured temperature range. The cell voltages of the single cells using the 4.7 wt.% GSC-coated cathode and an uncoated cathode, at a current density of 150 mA cm^{-2} and at different temperatures in the range 600–700 °C, are shown in Fig. 4(b). At 600 °C, the cell voltages of the GSC-coated cathode and the uncoated conventional cathode are 0.813 and 0.69 V, respectively. The enhancement of the cell performance at a low temperature after GSC coating is very surprising. The level of enhancement increases as the temperature decreases from 700 to 600 °C.

To identify the factors causing the performance enhancement, EIS analysis was carried out in the single cells. The linear relationship between $\ln(1/R_{\text{charge transfer}})$ and $1/T$ is presented in Fig. 5. As expected, increasing the measurement temperature results in a significant decrease in the charge transfer resistance, due to the increase in the electrochemical reaction rate at the electrode. Over the entire temperature range, the charge transfer resistance for the GSC-coated cathode is much lower than that for the uncoated cathode. In particular, the difference between the charge transfer resistance of the two cathodes is greater at lower temperatures. This is similar to the trend for the cell performance with temperature, as shown in Fig. 4(b). These data show that the reduced cathode polarization caused by the GSC coating is the primary cause of the enhancement of cell performance at low temperatures.

The lower charge transfer resistance after GSC coating makes the ORR at the cathode faster, and the cathode polarization lower. The activation energy of the charge transfer process at the cathode can be calculated using the slope obtained from the linear relationship between $\ln(1/R_{\text{charge transfer}})$ and $1/T$ [22]. The activation energies of the charge transfer process at the cathode for each single cell are 53.6 and 83.5 kJ mol^{-1} for the GSC-coated cathode and the uncoated cathode, respectively. The activation energy of the charge transfer process at the cathode is much lower after GSC coating. This result indicates that GSC on a conventional NiO cathode plays the role of a catalyst promoting the ORR at the cathode. It is known that GSC has many oxygen vacancies on its surface, and thus has a high catalytic activity [23,24], and these vacancies are an important factor in determining the ORR process. The oxygen vacancies of GSC are the carriers for O^{2-} transport via GSC particles to the triple phase boundary (TPB), at which the ORR occurs. Additionally, there are active sites that supply O^{2-} from the adsorption and dissociation of oxygen sources in carbonate melts or gas. Thus, O^{2-} provided supplementally from GSC on a conventional NiO cathode reduces the cathode polarization and promotes the ORR at the cathode.

To investigate the change in the cathode reaction process after GSC coating, symmetric cells using GSC-coated cathodes and uncoated cathodes were also constructed, and the cathode kinetics were examined at various partial pressures of O_2 and CO_2 in the temperature range 600–700 °C. The reaction orders of the two cells were calculated by linear regression from charge transfer resistance data at various partial pressures of O_2 and CO_2 [21]. The following correlations are used:

$$i \propto (\text{O}_2)^a (\text{CO}_2)^b \quad (1)$$

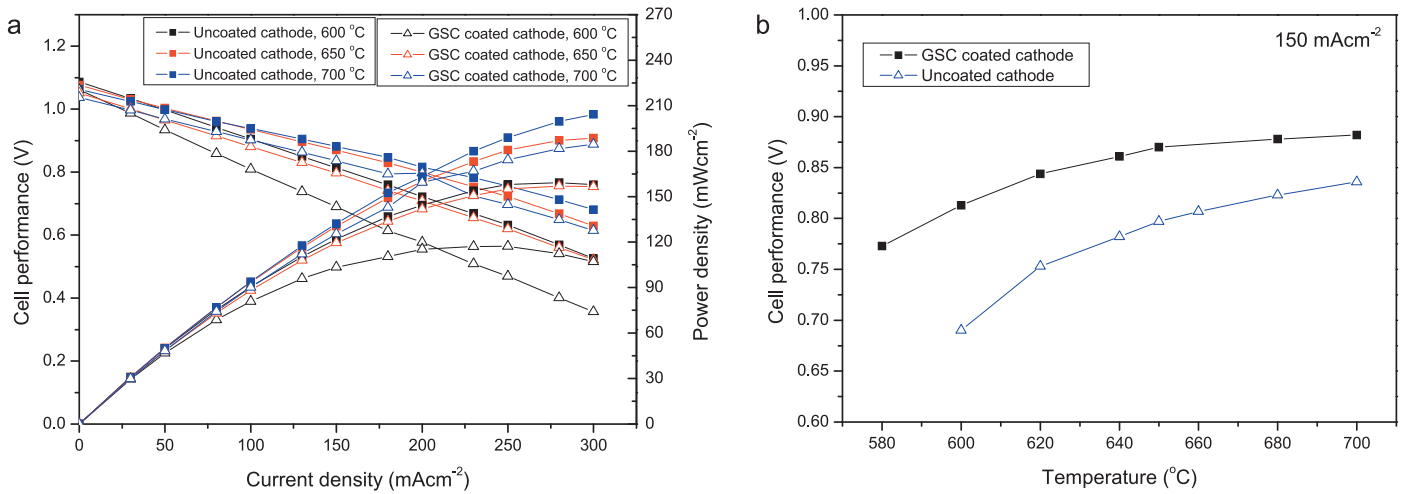


Fig. 4. (a) The j - V and j - P characteristics of single cells containing an uncoated cathode and a GSC-coated cathode at various operating temperatures, and (b) the voltages of single cells at a current density of 150 mA cm^{-2} at various operating temperatures.

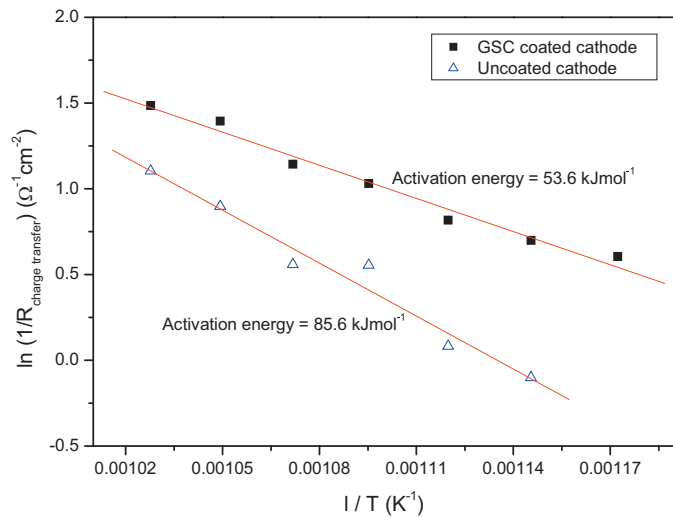


Fig. 5. The Arrhenius plots in cells containing a GSC-coated cathode or an uncoated cathode.

$$\frac{1}{R_{\text{charge transfer}}} \propto (\text{O}_2)^a (\text{CO}_2)^b \quad (2)$$

where i and $R_{\text{charge transfer}}$ are the exchange current density (mAcm^{-2}) and the charge transfer resistance ($\Omega \text{ cm}^2$), respectively. The cathodic reaction orders for O_2 (see Fig. 6) in cells using uncoated cathodes are 0.58, 0.36, 0.34, and 0.30 at 600, 620, 650, and 700 °C, respectively, while in cells using a GSC-coated cathode they are 0.28, 0.30, 0.28, and 0.28 at 600, 620, 650, and 700 °C, respectively. Generally, the ORR mechanisms in MCFCs are explained by three pathways—the peroxide, superoxide, and percarbonate pathways. These mechanisms assume that oxygen dissolves in the eutectic electrolyte in the form of peroxide, superoxide, or percarbonate ions [20,21,25,26]. Three pathways for the cathodic reaction in MCFCs are summarized in Table 2.

The theoretical cathodic reaction orders with respect to the O_2 partial pressure (exponent a) for the peroxide and superoxide mechanisms are 0.375 and 0.625, respectively. These values are higher than our experimental values. The low experimental values of the reaction order for oxygen are the result of the disproportionation reaction ($\text{O}_2^{2-} + 2\text{O}_2^- \leftrightarrow 2\text{O}^{2-} + 2\text{O}_2$) [25], a slow recombination reaction ($\text{O}^{2-} + \text{CO}_2 \leftrightarrow \text{CO}_3^{2-}$) [27], and the diffusion resistance of the reactant owing to the porous structure.

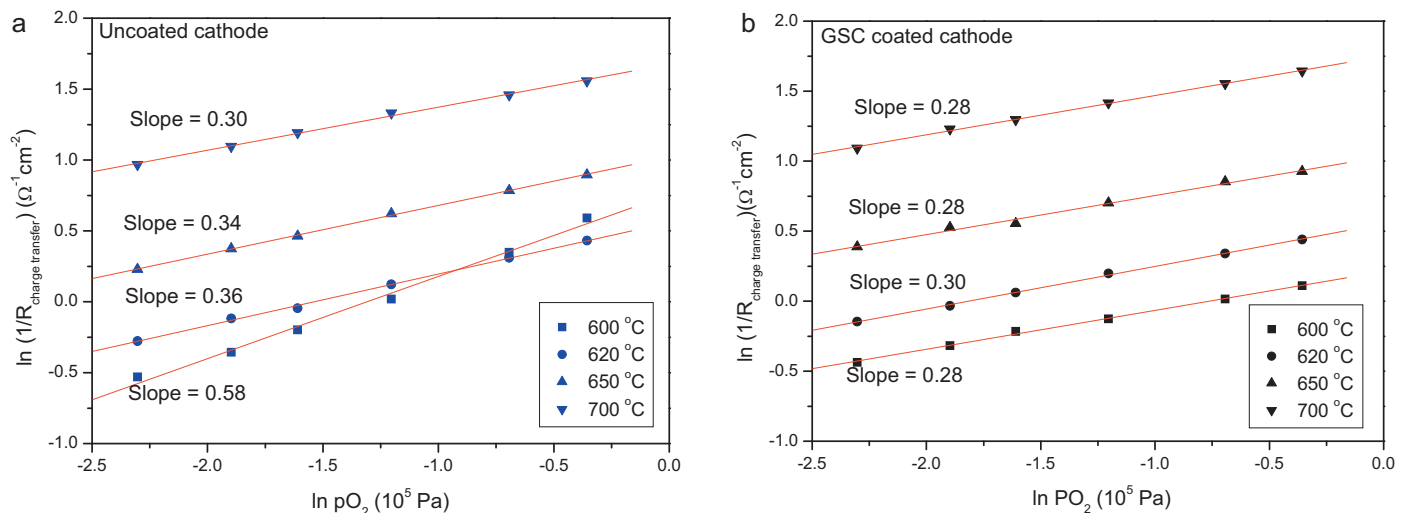


Fig. 6. The reaction orders with respect to O_2 in symmetric cells containing (a) an uncoated cathode, or (b) a GSC-coated cathode, at various operating temperatures.

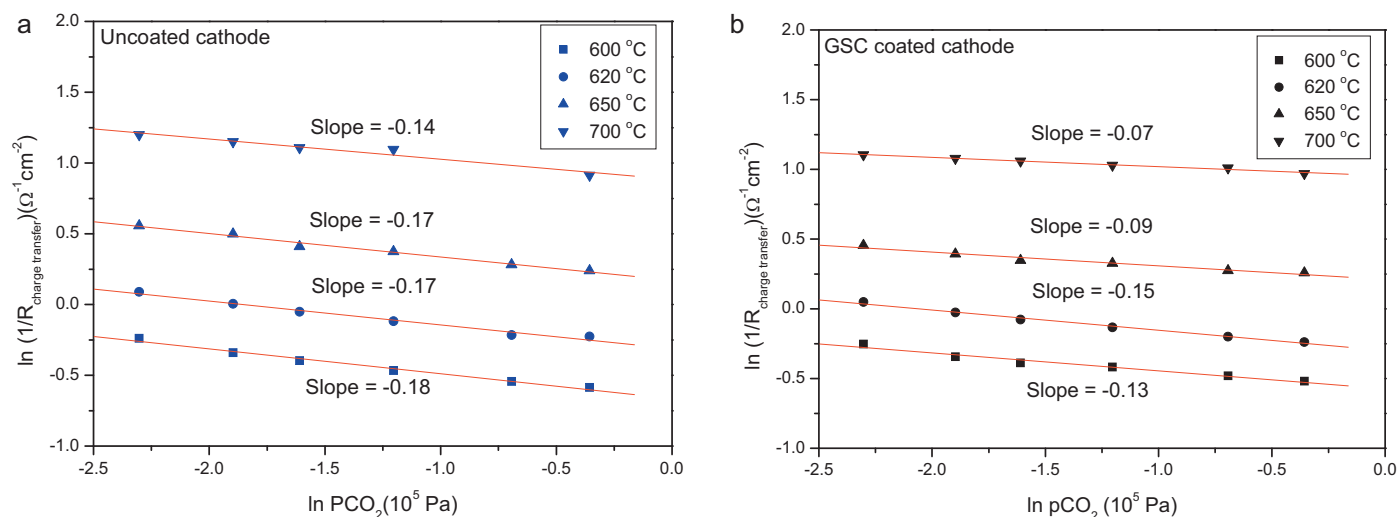


Fig. 7. The reaction orders with respect to CO_2 in symmetric cells containing (a) an uncoated cathode, or (b) a GSC-coated cathode, at various operating temperatures.

Table 2

Theoretical mechanisms of oxygen reduction in carbonate melts [25].

Peroxide pathway	$\text{O}_2 + 2\text{CO}_3^{2-} \leftrightarrow 2\text{O}_2^{2-} + 2\text{CO}_2$ $\text{O}_2^{2-} + 2\text{e}^- \leftrightarrow 2\text{O}^{2-}$ (rate-determining step, rds) $2\text{O}^{2-} + 2\text{CO}_2 \leftrightarrow 2\text{CO}_3^{2-}$ $i_0 \sim (\text{O}_2)^{0.375} (\text{CO}_2)^{-1.25}$
Superoxide pathway	$3\text{O}_2 + 2\text{CO}_3^{2-} \leftrightarrow 4\text{O}_2^- + 2\text{CO}_2$ $\text{O}_2^- + \text{e}^- \leftrightarrow \text{O}_2^{2-}$ (rds) $\text{O}_2^{2-} + 2\text{e}^- \leftrightarrow 2\text{O}^{2-}$ $2\text{O}^{2-} + 2\text{CO}_2 \leftrightarrow 2\text{CO}_3^{2-}$ $i_0 \sim (\text{O}_2)^{0.625} (\text{CO}_2)^{-0.75}$
Percarbonate pathway	$0.5\text{O}_2 + \text{CO}_3^{2-} \leftrightarrow \text{CO}_4^{2-}$ $\text{CO}_4^{2-} + \text{e}^- \leftrightarrow \text{CO}_3^{2-} + (\text{O}^-)$ (rds) $\text{O}^- + \text{CO}_2 + \text{e}^- \leftrightarrow \text{CO}_3^{2-}$ $i_0 \sim (\text{O}_2)^{0.375} (\text{CO}_2)^{-0.25}$

For the uncoated cathode, the reaction order changed from 0.57 to 0.30 over the temperature range 600–700 °C, indicating that the cathode reaction mechanism at the uncoated cathode shifts from the superoxide to the peroxide over this temperature range. In the case of the GSC-coated cathode, however, the reaction order does not change and is constant at 0.28 over the temperature range of 600–700 °C. This indicates that the peroxide reaction mechanism predominates at the GSC-coated cathode. According to Janowitz et al. [28], the cathodic reaction order for O_2 changes from 0.5 at 550 °C to 0.3 at 750 °C in Li/K eutectic melts, which is similar to our experimental results. Although many researchers have debated the ORR mechanism, it is generally known that the peroxide mechanism is predominant at high temperatures (≥ 700 °C) and that the superoxide mechanism is predominant at low temperatures [21,27–30]. Thus, the GSC coating makes the cathode reaction mechanism shift to the fast peroxide reaction mechanism at low temperatures. This shift explains why the GSC coating enhances the cell performance at low temperatures.

As shown in Fig. 7, the reaction orders for CO_2 in cells using uncoated cathodes are -0.18 , -0.17 , -0.17 , and -0.14 at 600, 620, 650, and 700 °C, respectively, and those in the cells using GSC-coated cathodes are -0.13 , -0.15 , -0.09 , and -0.07 at 600, 620, 650, and 700 °C, respectively. The theoretical reaction orders for the peroxide and superoxide mechanisms with respect to CO_2 are -1.25 and -0.75 , respectively, indicating that the cathodic reaction has a strong negative dependence on CO_2 . The reaction orders for CO_2 obtained experimentally are smaller than the theoretical values, and many researchers have reported similarly low experimental values [21,31]. According to the experimental results of Lu

and Selman [21], the low dependence on CO_2 concentration is a result of the net reaction at the electrode surface being the formation of two O^{2-} ions from O_2^- and three electrons (i.e., CO_2 does not participate in the reaction at the electrode surface), and the CO_2 reacting with the oxide ion in the melt to offset the negative dependence on the CO_2 concentration.

4. Conclusion

In this work, to improve cathode polarization at low temperatures, a perovskite material, GSC, is coated on a conventional lithiated NiO cathode. This modified cathode is to be used in MCFCs, because of its catalytic activity for the conversion of oxygen into oxygen ions, and its high electrical conductivity.

The enhancement in cell performance at 600 °C resulting from this GSC coating is impressive. Impedance analysis confirms that the improvement of the cell performance due to the GSC coating is a result of a dramatic reduction in the charge transfer resistance at low temperatures. From impedance analysis in symmetric cells, it is confirmed that the reaction mechanism at the cathode after GSC coating is predominantly the peroxide reaction mechanism, even at low temperatures. This fast reaction mechanism usually takes place at high temperatures at conventional cathodes. Thus, the GSC coating enhances the cell performance at low temperatures because it leads to fast oxygen reduction and low cathode polarization. The stable operating period of 2200 h for a single cell using a GSC-coated cathode indicates that these cathodes are chemically stable and are not degraded by the carbonate electrolyte. These results indicate that GSC-coated cathodes are a very promising candidate for use in MCFCs operated at low temperatures.

Acknowledgment

This research was supported by a New & Renewable Energy of the Korea Institute of Energy Technology Evaluation and Planning (KETEP) Grant funded by the Korean government Ministry of Knowledge Economy (Project No. 2008-NFC12J0431102010).

References

- [1] B.H. Ryu, I.G. Jang, K.H. Moon, J. Han, T.-H. Lim, J. Fuel Cell Sci. Technol. 3 (2006) 389–395.
- [2] J.-E. Kim, K.Y. Patil, J. Han, S.P. Yoon, S.W. Nam, T.-H. Lim, S.-A. Hong, H. Kim, H.C. Lim, Int. J. Hydrogen Energy 34 (2009) 9227–9232.

- [3] H.-K. Seo, Y.-C. Eom, Y. Chun, S.-D. Lee, J.-H. Gu, J. Power Sources 166 (2007) 165–171.
- [4] K. Tanimoto, M. Yanagida, T. Kojima, Y. Tamiya, H. Matsumoto, Y. Miyazaki, J. Power Sources 72 (1998) 77–82.
- [5] H. Okawa, J.-H. Lee, T. Hotta, S. Ohara, S. Takahashi, T. Shibahashi, Y. Yamamasu, J. Power Sources 131 (2004) 251–255.
- [6] S. Frangini, J. Power Sources 182 (2008) 462–468.
- [7] J.Y. Youn, S.P. Yoon, J. Han, S.W. Nam, T.-H. Lim, S.-A. Hong, K.Y. Lee, J. Power Sources 157 (2006) 121–127.
- [8] S. Freni, E. Passalacqua, F. Barone, Int. J. Energy Res. 21 (1997) 1061–1070.
- [9] C. Xia, W. Rauch, F. Chen, M. Liu, Solid State Ionics 149 (2002) 11–19.
- [10] G. Zhang, X. Dong, Z. Liu, W. Zhou, Z. Shao, W. Jin, J. Power Sources 195 (2010) 3386–3393.
- [11] S.P. Jiang, Solid State Ionics 146 (2002) 1–22.
- [12] B. Liu, Y. Zhang, L. Zhang, Int. J. Hydrogen Energy 34 (2009) 1008–1014.
- [13] K.T. Lee, A. Manthiram, J. Electrochem. Soc. 153 (2006) A794–A798.
- [14] S. Huang, C. Peng, Z. Zong, J. Power Sources 176 (2008) 102–106.
- [15] J. Chen, F. Liang, B. Chi, J. Pu, S.P. Jiang, L. Jian, J. Power Sources 194 (2009) 275–280.
- [16] J. Chen, F. Liang, L. Liu, S. Jiang, B. Chi, J. Pu, J. Li, J. Power Sources 183 (2008) 586–589.
- [17] C.R. Dyck, Z.B. Yu, V.D. Krstic, Solid State Ionics 171 (2004) 17–23.
- [18] H. Devianto, S.P. Yoon, S.W. Nam, J. Han, T.-H. Lim, J. Power Sources 159 (2006) 1147–1152.
- [19] P. Ganesan, H. Colon, B. Haran, B.N. Popov, J. Power Sources 115 (2003) 12–18.
- [20] L. Giorgi, M. Carewska, S. Scaccia, E. Simonetti, E. Giacometti, R. Tulli, Int. J. Hydrogen Energy 21 (1996) 491–496.
- [21] S.H. Lu, J.R. Selman, J. Electroanal. Chem. 333 (1992) 257–271.
- [22] A. Barbucci, R. Bozzo, G. Cerisola, P. Costamagna, Electrochim. Acta 47 (2002) 2183–2188.
- [23] Y. Takeda, H. Ueno, N. Imanishi, O. Yamamoto, N. Sammes, M.B. Phillipps, Solid State Ionics 86–88 (1996) 1187–1190.
- [24] H.-D. Wiemhofer, H.-G. Bredes, U. Nigge, Solid State Ionics 175 (2004) 93–98.
- [25] C.Y. Yuh, J.R. Selman, J. Electrochem. Soc. 138 (1991) 3642–3648.
- [26] F.J. Perez, D. Duday, M.P. Hierro, C. Gomez, M.T. Romero, J.A. Casais, M.J. Alonso, L.D. Martinez, J. Power Sources 86 (2000) 309–315.
- [27] S.H. Lu, J.R. Selman, J. Electrochem. Soc. 137 (1990) 1125–1130.
- [28] K. Janowitz, M. Kah, H. Wendt, Electrochim. Acta 45 (1999) 1025–1037.
- [29] R.W. Reeve, A.C.C. Tseung, J. Electroanal. Chem. 403 (1996) 69–83.
- [30] W.H.A. Peelen, K. Hemmes, J.H.W. de Wit, J. Electroanal. Chem. 470 (1999) 39–45.
- [31] J.A. Prins-Jansen, K. Hemmes, J.H.W. de Wit, Electrochim. Acta 42 (1997) 3601–3618.